JACS
JOURNAL OF THE AMERICAN CHEMICAL SOCIETY

COMMUNICATION

pubs.acs.org/JACS

The Fast and the Slow: Folding and Trapping of λ_{6-85}

Maxim B. Prigozhin[†] and Martin Gruebele[*,†,‡]

[†]Department of Chemistry and [‡]Department of Physics and Center for Biophysics and Computational Biology, University of Illinois, Urbana, Illinois 61801, United States

Supporting Information

ABSTRACT: Molecular dynamics simulations combining many microsecond trajectories have recently predicted that a very fast folding protein like lambda repressor fragment λ_{6-85} D14A could have a slow millisecond kinetic phase. We investigated this possibility by detecting temperature-jump relaxation to 5 ms. While λ_{6-85} D14A has no significant slow phase, two even more stable mutants do. A slow phase of λ_{6-85} D14A does appear in mild denaturant. The experimental data and computational modeling together suggest the following hypothesis: λ_{6-85} takes only microseconds to reach its native state from an extensively unfolded state, while the latter takes milliseconds to reach compact β-rich traps. λ_{6-85} is not only thermodynamically but also kinetically protected from reaching such "intramolecular amyloids" while folding.

Small proteins have become important benchmarks for folding theory[1] and simulation.[2] Single- and multitrajectory simulations now make easily testable predictions about folding rates and stabilities.[2−4] Lambda repressor fragments, originally a paradigm for stability measurements[5] and later adapted for NMR and temperature-jump (T-jump) kinetics,[6,7] have become the largest "small" platforms for computational studies:[2,8] 80 amino acids in five helices for the λ_{6-85} fragment. Experimentally, slower-folding mutants are assigned as apparent two-state folders,[6,9] whereas sub-20 μs mutants are assigned as downhill or incipient downhill folders.[7,10] The latter assignment is based on the 2 μs "molecular phase" observed only upon stabilization of the native state and attributed to direct observation of the barrier crossing.[7,11] A recent long-trajectory simulation confirmed the low barriers determined experimentally ($1.5k_BT$ for λD14A in Table 1).[8]

Experimental analyses of two reaction coordinates[9] and multiple probes[12] using alanine-rich and -poor mutants of λ_{6-85} demonstrated that even apparent two-state folders require $\geq$2 reaction coordinates and >2 states for a full description. In addition, λ_{6-85} has a propensity to adopt an extended structure (here abbreviated PP/β because it is found in polyproline helices or β strands) at high temperature and in mild denaturant.[13]

Indeed, a rich energy landscape structure has been predicted by a Markov state analysis of multiple λ_{6-85} folding trajectories. For the λD14A mutant (Table 1), Bowman et al.[2] carried out relaxation simulations starting with equal populations in the denatured microstates. They found two <10 μs phases, in general agreement with T-jump experiments, but also a much slower $\geq$1 ms phase. The slow phase is present in simulations without denaturant and is associated with compact β-rich denatured states; it disappears only when the β structural ensemble is removed from the calculation.

Table 1. λ-Repressor Nomenclature, Mutations from Wild Type, and Melting Temperatures (Rounded to the Nearest °C) As Determined by Fluorescence Wavelength Shifts

name	mutations	T_m (°C)
λQ33Y	Y22W, Q33Y, G46A, G48A	70 ± 0.5
λsQ33Y	Y22W, Q33Y	70 ± 0.5
λD14A	D14A,Y22W,Q33Y,G46A, G48A	68 ± 0.5
λnQ33Y	Y22W, Q33Y, A37G, A49G	53 ± 0.5
λsA49G	Y22W, A37G, A49G	48 ± 0.5

Bowman et al. offered several possible explanations for the calculated slow phase: it may have been missed by laser T-jump experiments, which usually extend to <0.5 ms; the slow phase may represent very slow folding of λ_{6-85} in denaturant, as previously seen by experiment;[14] or the force field they used may overemphasize β-sheet stability.

We have continued the experiment−simulation dialogue by carrying out new 5 ms T-jump measurements on alanine-rich and -poor mutants of λ_{6-85}. We show that all of the above explanations apply: We detected no significant slow phase for λD14A, so the force field or the equal-population initial condition overestimates the β-sheet propensity for this mutant. However, we detected a slow phase for two even more stable λ_{6-85} mutants, λQ33Y and λsQ33Y, proving that slow interconversion between structural ensembles of λ_{6-85} can occur without denaturant. Moreover, λD14A also begins to show a slow phase in mild denaturant. The computational suggestion that compact β-rich traps result in slow dynamics is thus plausible, although λ_{6-85} still refolds in microseconds from the extensively unfolded state if it can avoid such traps. Our results highlight once again the importance of thermodynamic tuning when comparing experiment and computation, because small free energy discrepancies (δG) can produce large population differences ($\sim e^{-\delta G/RT}$).

λ_{6-85} mutant stability differs by fluorescence and CD detection. We selected a set of λ-repressor mutants spanning a wide range of stabilities (Table 1). Nominal melting temperatures (T_m) were determined from two-state fits with linear baselines (Figure 1). We reproduced the circular dichroism (CD) melting temperatures [see the Supporting Information (SI)].[9] New measurements of T_m by fluorescence wavelength shifts, which are better correlated with tryptophan fluorescence detected during T-jumps, yielded a different stability ranking. λD14A is ranked

Received: September 27, 2011
Published: November 08, 2011

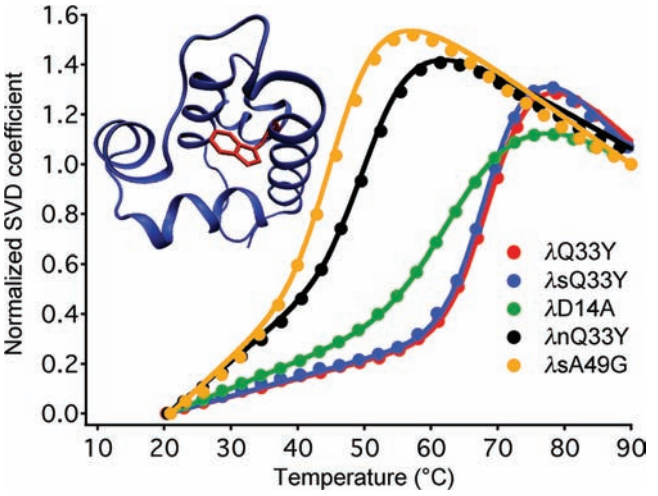

Figure 1. Thermal denaturation of the λ-repressor mutants in Table 1. The singular value decomposition (SVD) shown here represents the wavelength shift of the W22 fluorescence spectrum (raw data are given in the SI). The inset shows W22 in the crystal structure of λQ33Y.[15]

most stable by CD[9] but less stable than λQ33Y and λsQ33Y by wavelength shift (Figure 1). Such differences indicate a breakdown of two-state behavior.

The mutants were divided into three categories on the basis of fluorescence-detected thermal stability. λQ33Y and λsQ33Y were the most stable variants, with melting temperatures of 70 °C. The broader melting curve of λD14A occupied an intermediate stability range. λnQ33Y and λsA49G mutants were the least stable of the studied proteins.

Only the two most stable λ-repressor fragments have a significant slow-phase amplitude. We studied the slow relaxation phase of λ-repressor variants by collecting ∼5 ms of tryptophan fluorescence decays after the T-jump. The tryptophan decay lifetime is sensitive to folding. Individual decays with ∼3 ns lifetime were sampled at 100 ps intervals for 12.5 ns per decay, yielding a total of ∼400 000 decays per kinetic trace. Each jump was then reproduced 60 times. Figure 2 shows the combined results for three of the mutants binned into 1.25 μs intervals. The function $\chi(t)$ normalizes the tryptophan fluorescence decay time as a folding probe from $\chi = 1$ (shorter lifetime for all Y33 mutants) to $\chi = 0$ (longer lifetime for all Y33 mutants). All data at $t > 1$ μs were fitted using a double-exponential function with the baseline fixed at zero. With that constraint and the signal-to-noise ratio, slow phases (<10% of the fast-phase amplitude and slower than a few ms) were not discernible in our experiments. The fast initial phase has been discussed in detail elsewhere.[7,15,16] The largest slow phases (e.g., Figure 2A) could be fitted by observed relaxation times (τ) of 1.2−1.6 ms, and this range also provided good fits for small-amplitude slow phases (if any) of other mutants (for more information, including correction of baselines for recooling and tryptophan photobleaching, see the SI).

λD14A, which was investigated computationally by Bowman et al., showed only a ≤10% slow-phase amplitude, nearly within experimental error (Figure 2B and Table 2). The more stable (by fluorescence melt) λQ33Y and λsQ33Y had by far the largest A_{slow}/A_{fast} ratio among all of the studied mutants (Figure 1A, Table 2, and the SI). Moreover, the amplitude of the slow phase switched when the temperature was increased. This can be explained by a model with at least two non-native states having

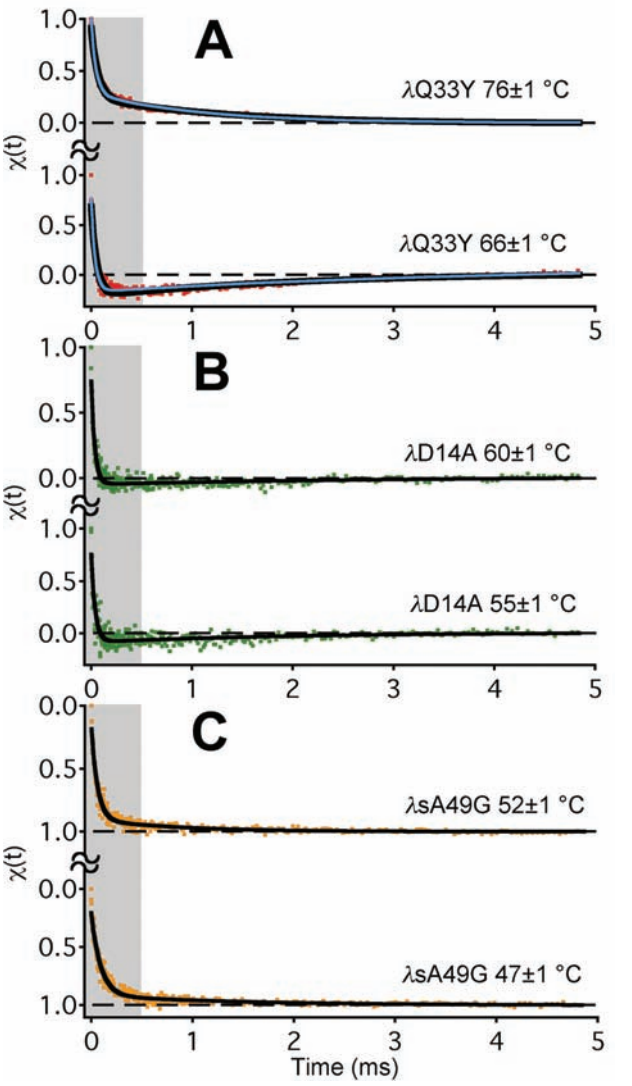

Figure 2. T-jump kinetics of λ-repressor mutants detected by tryptophan fluorescence decay, with double-exponential fits in black. The global model fits are shown as blue curves in (A). Traces were normalized from 1 (fast fluorescence decay) to 0 (slow decay). The fast phase (gray areas) was investigated previously,[7,9,16] so the ms scale is emphasized here.

Table 2. Ratios of Amplitudes of Slow- and Fast-Folding Phases in λ-Repressor Mutants Having Different Stabilities

name	T (±1 °C)	A_{slow}/A_{fast}
λQ33Y	76	0.37 ± 0.02
	66	−0.27 ± 0.03
λD14A	60	−0.08 ± 0.08
	55	−0.11 ± 0.09
λsA49G	52	0.1 ± 0.4
	47	0.1 ± 0.2

different tryptophan lifetimes (see below). The glycine-rich and least stable variants, λsA49G and λnQ33Y, showed ≤10% slow phases within experimental error (Figure 2C, Table 2, and the SI).

Denaturant produces a slow phase in the D14A mutant. Bowman et al. proposed that the simulation might mimic mild denaturant

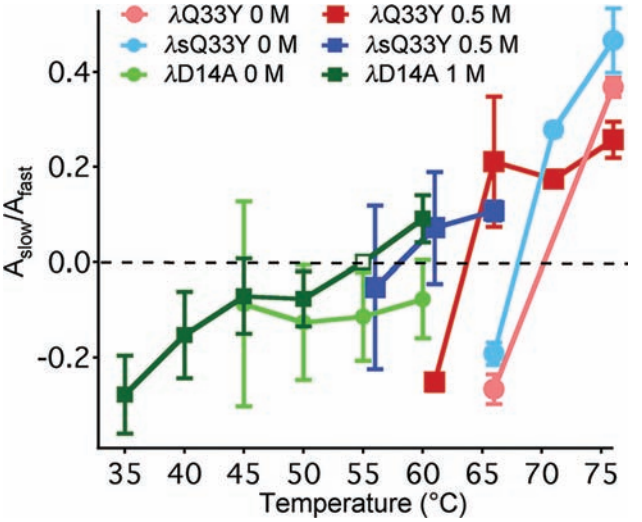

Figure 3. Dependence of the A_{slow}/A_{fast} ratio on temperature with and without GuHCl. (□: fixed.)

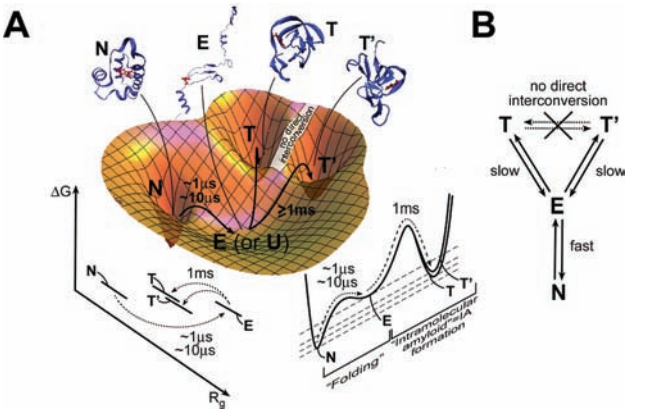

Figure 4. Folding of λ_{6-85} mutants along reaction coordinates related to compactness (R_g) and non-native secondary structure content. (A) Free energy landscape. The folding process per se from an extensively unfolded state E (or U) to N is fast. E can also convert slowly to compact non-native states T and T′. Suggested structures are from refs 2 and 15 (N). (B) Kinetic scheme. T and T′ interconvert indirectly through E, which is in rapid equilibrium with N.

conditions. T-jump experiments were also conducted at low concentrations of guanidine hydrochloride (GuHCl), which was previously reported to induce the formation of the PP/β structure in λ-repressor fragments.[13] Our kinetics experiments showed that 0.5 M GuHCl destabilizes the λ_{6-85} series by ~10 °C. The range of the A_{slow}/A_{fast} ratio did not increase in GuHCl for the most stable mutants; they are "maxed out". However, λD14A showed an increased range of A_{slow}/A_{fast} in 1 M GuHCl, beginning to resemble the more stable mutants (Figure 3). The least stable mutant, λsA49G, does not completely fold at room temperature in just 0.5 M GuHCl (see the SI). Thus, addition of the denaturant does produce slow kinetics for the mutants of intermediate stability, consistent with the suggestion by Bowman et al. that force-field error in the all-atom simulations may correspond to experimental conditions in mild denaturant.

The small millisecond phase of λD14A relative to λQ33Y and λsQ33Y is a genuine indicator that slow dynamics is less important in λD14A and not simply a result of tryptophan fluorescence sometimes being insensitive to slow phases. There is strong evidence that W22 fluorescence can monitor the slow phase whenever it is present in these three mutants. Oas and co-workers suggested that the Q33Y mutation substantially increases the quenching of tryptophan upon folding (private communication), and the Y33—W22 interaction in the native state has been verified by X-ray crystallography of the λQ33Y mutant.[15] The Y33—W22 interaction is equally present in all three mutants on the basis of the large fluorescence changes observed upon melting (Figure 1 and the SI).

A low-resolution landscape model. The unusual result is that the most highly stabilized forms of λ_{6-85} are most likely to get stuck in β-sheet traps, assuming that our slow experimental phase has the same origin as the ≥1 ms phases simulated by Bowman et al. With two very different time scales (~10 μs vs ~1 ms for the most stable mutants), our data can be explained by a low-resolution model with three or more states. We will focus on a simple global model consistent with all of the experimental and computational observations to date. The model suggests a specific new hypothesis for future testing.

λ_{6-85} with oxidized methionines has been used to mimic the denatured state under native conditions.[17] It exhibits strong helical propensity for residues 6—20 (centered on helix 1) and reduced flexibility for residues 50—83 (centered on helix 4) but no evidence for a stable PP/β structure. Thus, the unfolded λ-repressor does not necessarily form the compact sheet structure proposed by simulation under native solvent conditions. On the other hand, we recently reported several new mini-proteins containing only λ-repressor helices 1 and 4 connected by a linker.[18] One (λ_{blue1}) has a CD spectrum, denaturation curve, and T-jump kinetics consistent with a cooperatively folding two-helix bundle. The slightly different λ_{blue3} sequence has a CD spectrum peaked at 215 nm, consistent with β-sheet content.[18] We also observed a CD signature consistent with a PP/β structure in several λ-repressor fragments subjected to combinations of high temperature and mild denaturant.[13] Thus, the PP/β structure is not much higher in free energy than the native α-helical secondary structure.

We fitted the data in Figure 2A with several three-state models (see the SI). The free energy landscape most consistent with experiment (observed tryptophan lifetime changes) and thermodynamic expectations (extensively unfolded states should have lower free energy than compact states at high temperature) is shown in Figure 4A and depicted as a kinetic scheme in Figure 4B. The NET model is consistent with both experiment and simulation. The fits to the global model (blue curves in Figure 2A) closely match the experimental kinetics. The computed structure we suggest as representative for E in Figure 4A has a 0.99 computed probability of reaching N before reaching T.[2] This is consistent with a rate ratio of 100:1 or a relaxation time ratio of 10 μs:1 ms, close to experimental observation.

In the NET model, the extensively unfolded state E interconverts in microseconds with the native α-helical state N. This process is what one ordinarily considers as protein folding. In addition, E interconverts in milliseconds with traps such as T or T′. We fitted such traps as a single kinetic state because our fluorescence probe cannot distinguish them.

Kinetic traps of various types are known for many proteins,[19] but the simulations of Bowman et al. make very specific structural predictions in addition to predicting a millisecond relaxation time: different traps T and T′ resemble each other in compactness and high β-sheet content but differ in the detailed

arrangement of the sheets. The slow interconversion of T and T′ is thus explained because their non-native secondary structure has to be unmade via the extensively unfolded state E. Once E is reached, it very rapidly interconverts with N. Therefore, N is sampled many times on the time scale of T and T′ interconversion. In our view, the native state N is thus not so much a "hub" but is simply easily reached from E, if we distinguish the N ⇄ E "folding process proper" from the E ⇄ T,T′ misfolding process.

Hypothesis. We suggest the following hypothesis to explain the structures seen by Bowman et al. as well as the slow phase observed experimentally only for the most stable λ_{6-85} mutants: Proteins whose hydrophobic interactions strongly favor compact states are prone to form compact β-rich traps or "intramolecular amyloids" (IAs). There is evidence for a PP/β structure in monomeric denatured states of many proteins.[13,20] Such non-native secondary structure could get locked in when proteins rapidly become compact during folding, especially under mildly denaturing conditions. In particular, large proteins with many nonlocal options for hydrophobic contacts and β-strand formation might be more likely to form IAs in need of rescue by chaperones. Direct structural evidence for IAs could come from two-dimensional IR kinetics studies. IAs are complementary to a phenomenon observed for some proteins with a β-rich native state: formation of non-native helical traps facilitated by favorable local interactions.[21]

Proteins have some kinetic and thermodynamic protection from IAs: Kinetically, the extensively unfolded state E converts much more rapidly to N than to T, in analogy to the large barrier separating real amyloid aggregates from denatured proteins and native states. Thermodynamically, T still ends up higher in free energy than N (unlike real amyloid aggregates; see the model fit in the SI). From an energy landscape perspective, one would say that fast folding λ-repressors have a glass transition temperature T_g dangerously close to the folding temperature T_f[22] but still end up getting stuck in traps only temporarily.

■ ASSOCIATED CONTENT

Supporting Information. Methods, additional figures showing data for all mutants, and tables containing fitting parameters. This material is available free of charge via the Internet at http://pubs.acs.org.

■ AUTHOR INFORMATION

Corresponding Author
mgruebel@illinois.edu

■ ACKNOWLEDGMENT

Funding was provided by NIH Grant R01 GM093318. M.B.P. was also supported by a Chemistry Department Fellowship. We thank G. R. Bowman and V. Pande for comments and additional simulation data.

■ REFERENCES

(1) Portman, J. J.; Takada, S.; Wolynes, P. G. *J. Chem. Phys.* **2001**, *114*, 5069.
(2) Bowman, G. R.; Voelz, V. A.; Pande, V. S. *J. Am. Chem. Soc.* **2011**, *133*, 664.
(3) Piana, S.; Sarkar, K.; Lindorff-Larsen, K.; Guo, M.; Gruebele, M.; Shaw, D. E. *J. Mol. Biol.* **2011**, *405*, 43.
(4) Noé, F.; Schütte, C.; Vanden-Eijnden, E.; Reich, L.; Weikl, T. R. *Proc. Natl. Acad. Sci. U.S.A.* **2009**, *106*, 19011.
(5) Hecht, M. H.; Sturtevant, J. M.; Sauer, R. T. *Proc. Natl. Acad. Sci. U.S.A.* **1984**, *81*, 5685.
(6) Huang, G. S.; Oas, T. G. *Biochemistry* **1995**, *34*, 3884.
(7) Yang, W. Y.; Gruebele, M. *Nature* **2003**, *423*, 193.
(8) Lindorff-Larsen, K.; Piana, S.; Dror, R. O.; Shaw, D. E. *Science* **2011**, *334*, 517.
(9) Yang, W. Y.; Gruebele, M. *Biochemistry* **2004**, *43*, 13018.
(10) DeCamp, S. J.; Naganathan, A. N.; Waldauer, S. A.; Bakajin, O.; Lapidus, L. J. *Biophys. J.* **2009**, *97*, 1772.
(11) Liu, F.; Gruebele, M. *J. Chem. Phys.* **2009**, *131*, No. 195101.
(12) Ma, H.; Gruebele, M. *Proc. Natl. Acad. Sci. U.S.A.* **2005**, *102*, 2283.
(13) Yang, W.; Larios, E.; Gruebele, M. *J. Am. Chem. Soc.* **2003**, *125*, 16220.
(14) Yang, W. Y.; Gruebele, M. *Phil. Trans. R. Soc., Ser. B* **2005**, *43*, 13018.
(15) Liu, F.; Gao, Y.-G.; Gruebele, M. *J. Mol. Biol.* **2009**, *397*, 789.
(16) Yang, W.; Gruebele, M. *Biophys. J.* **2004**, *87*, 596.
(17) Chugha, P.; Oas, T. G. *Biochemistry* **2007**, *46*, 1141.
(18) Prigozhin, M. B.; Sarkar, K.; Law, D.; Swope, W. C.; Gruebele, M.; Pitera, J. *J. Phys. Chem. B* **2011**, *115*, 2090.
(19) Oliveberg, M.; Wolynes, P. G. *Q. Rev. Biophys.* **2005**, *38*, 245.
(20) Fitzkee, N. C.; Rose, G. D. *Proc. Natl. Acad. Sci. U.S.A.* **2004**, *101*, 12497.
(21) Hamada, D.; Segawa, S.; Goto, Y. *Nat. Struct. Biol.* **1996**, *3*, 868.
(22) Socci, N. D.; Onuchic, J. N.; Wolynes, P. G. *Proteins: Struct., Funct., Genet.* **1998**, *32*, 136.